Partially-Filled Half-Mode Substrate Integrated Waveguide Leaky-Wave Antenna for 24-GHz Automotive Radar

Kamil Yavuz Kapusuz, *Student Member, IEEE*, Andres Vanden Berghe, Sam Lemey, *Member, IEEE*, and Hendrik Rogier, *Senior Member, IEEE*

***Abstract*—A novel highly efficient leaky-wave antenna (LWA), based on a periodic set of holes created in a half-mode substrate integrated waveguide (SIW), is conceived for automotive radar. The computer-aided design of this partially-filled SIW (PFSIW) LWA is carried out using a full-wave electromagnetic simulator. As a proof-of-concept, an LWA prototype having a plate size of 15x126 mm^2 is fabricated through a standard low-cost printed circuit board (PCB) manufacturing process. Our manufactured prototype yields more than 25% impedance bandwidth, targeting the 24 GHz automotive short-range-radar band. Moreover, the measured peak gain and total antenna efficiency reach up to 15.5 dBi and 85% at 24 GHz. Furthermore, the main radiating direction steers continuously from 38° to 58° with an average half-power beamwidth of 12° when the operating frequency changes from 22 GHz to 26 GHz. In comparison, a 160-mm-long dielectric-filled SIW LWA yields a measured scanning range of 49° and a total antenna efficiency of 43.8%, whereas an 80.3-mm-long air-filled SIW LWA exhibits a measured scanning range of 9° and a total antenna efficiency of 80%. Therefore, PFSIW technology provides an optimal trade-off between DFSIW and AFSIW for the envisaged short-range automotive radar application.**

***Index Terms*—Air-filled, automotive radar, dielectric-filled, frequency scanning antenna, leaky-wave antenna (LWA), partially-filled, substrate integrated waveguide (SIW).**

I. Introduction

EFFICIENT and stable automotive radars are essential for autonomous driving systems to reduce risky and dangerous behaviors [1]. These sensors should be compact, while exhibiting a stable high-gain steerable-beam capability to identify moving objects at short range even where the relative position of the object is not known [2]. Moreover, the system's dimensions should enable invisible integration into different car types. Furthermore, new cost-efficient fabrication technologies should be developed to pervasively co-integrate antenna systems into the vehicles. Consequently, to reduce the number of casualties in daily traffic, antennas in automotive radars have to be improved with respect to cost and performance.

Frequency scanning antennas in substrate integrated waveguide (SIW) technology have been gaining a lot of interest in radar systems because of their economical beam scanning, easy and low-cost fabrication, and their potential for unobtrusive and robust integration. Yet, the dielectric losses in conventional dielectric-filled SIW (DFSIW) technology inevitably limit radiation efficiency, making it less suited for commercial automotive radar, such as short-range radar (SRR) at 24 GHz, 77 GHz and 94 GHz, targeting highly efficient antenna systems in a compact footprint. As a solution, air-filled SIW (AFSIW) was introduced to mitigate the dielectric loss of the DFSIW topology by replacing the dielectric substrate material by air [3]–[5]. However, this reduces the frequency scanning capability to such extent that the endfire direction cannot be reached. Alternatively, exploiting partially-filled SIW (PFSIW) technology [6] may alleviate the dielectric loss while facilitating wide frequency scanning.

This letter proposes a new partially-filled half-mode SIW (HM-SIW) leaky-wave antenna (LWA), operating in the [22-26] GHz band. This novel antenna topology yields: (i) a considerable efficiency enhancement and a small form factor that is compatible with its dielectric-filled counterpart, (ii) a significantly improved scanning range compared to the air-filled topology, (iii) low fabrication and beam steering costs and (iv) an excellent antenna/platform isolation. Consequently, the proposed antenna topology provides an optimal trade-off between DFSIW and AFSIW for the envisaged short range automotive radar.

Several technologies to reach an optimum solution in terms of antenna performance and manufacturing cost in K-Band have been developed in the past decades, including microstrip [7], [8], lens [9]–[13] and waveguide [14]–[16] topologies. [7] proposes a microstrip-fed endfire angled dipole array. Although this design yields a promising continuous beam steering solution, expensive and lossy phase shifters are necessary, which must be interconnected with low insertion loss. [8] presents a microstrip periodic leaky-wave topology, offering efficient and economical beam scanning. Yet, the inherent losses of microstrip technology reduce the radiation efficiency. [9]–[13] rely on planar multilayer lens-based phased arrays. Even though these solutions are relatively compact, exploiting multilayer PCB technology makes the antenna construction expensive. Furthermore, beam steering is restricted to predefined angles without possibility of continuous beam scanning. [14]–[16] propose traveling-wave phased arrays implemented in SIW technology. These solutions feature a substantial cost reduction owing to their single-RF-layer antenna topology and they enable frequency scanning. Yet, they suffer from low antenna efficiency due to high dielectric

Manuscript received October 13, 2020; accepted November 9, 2020. Date of publication ; date of current version . This work was partially supported by the European Research Council through ATTO: A new concept for ultrahigh capacity wireless networks under Grant 695495.

The authors are with the IDLab-Electromagnetics Group, Department of Information Technology, Ghent University-IMEC, Technologiepark 126, Ghent B-9052, Belgium. (e-mail: kamilyavuz.kapusuz@ugent.be; andres.vandenberghe@ugent.be; sam.lemey@ugent.be; hendrik.rogier@ugent.be).

This article has been accepted for publication in a future issue of this journal, but has not been fully edited. Content may change prior to final publication. Citation information: DOI 10.1109/LAWP.2020.3038201, IEEE Antennas and Wireless Propagation Letters

and conductor losses.

This letter is organized as follows. Section II outlines all design aspects of the novel antenna topology and its implementation technology. Section III proposes the PFSIW technology, demonstrating its advantages over DFSIW and AFSIW solutions. A fabricated prototype is validated in Section IV. Finally, a conclusion is drawn in Section V.

II. Antenna Topology, Design and Manufacturing

A linearly polarized partially-filled HM-SIW LWA [Fig. 1] is designed for SRR in the [22–26] GHz band, compliant with the standards of the Federal Communications Commission (FCC) [17]. A total antenna efficiency over 80% and a return loss larger than 10 dB (with respect to 50 Ω) are imposed over the entire operating band. Moreover, a steerable main beam is required to point the radiation pattern maximum towards the angle that corresponds to the object direction. Finally, a low-cost fabrication procedure that provides robust performance and high efficiency in realistic deployment scenarios is desired to remain competitive with current state-of-the-art solutions.

Therefore, the topology in Fig. 1(a) is adopted, consisting of two conductive layers (Layer 1 and Layer 3) and one dielectric layer (Layer 2). Layers 1 and 3, realized by edge-plated low-cost 1.0-mm-thick-FR4 substrates (ϵ_r = 4.3, tanδ = 0.024), implement the top and bottom conducting boundaries for the middle dielectric layer (Layer 2), consisting of a low-loss 0.5-mm-thick-Rogers RO4350B substrate (ϵ_r = 3.66, tanδ = 0.0031) [Fig. 1(c)]. First, in this layer, a three-sections' transition from the SMA probe to the half-mode LWA [Fig. 1(b)], inspired by an SIW transition on a high-to-low dielectric constant substrate introduced in [18], is created to achieve matching over the band of operation. The flexible and straightforward grounded coplanar waveguide (GCPW) feed facilitates high isolation and enables compact integrated circuit (IC) assemblies, as opposed to the rather bulky metallic waveguide feed. The triangular-shaped dielectric substrate [Fig. 1(b)] tapers from a full-mode dielectric SIW into the HM-SIW LWA. Then, to control the leaky wave's propagation characteristic and to reduce the substrate loss in the antenna [19], a partially-filled HM-SIW waveguide section is realized in the dielectric layer by introducing an array of milled-out cylindrical air holes with diameter d_h and periodicity s_h [Fig. 1(b)], after which through-plated vias create the HM-SIW's side walls with diameter d and periodicity s. Finally, all layers are assembled by 1.4-mm-diameter alignment pins and fixations, to guarantee sufficient electrical contact and to provide accurate alignment.

This topology is optimized to generate highly-directive steerable beams over a broad scan range. First, a full-mode rectangular SIW is created. The width and thickness of the cross-section are dimensioned such that only its fundamental quasi-TE_{10} mode is propagating. Next, an HM-SIW exciting leaky waves is implemented by cutting the SIW waveguide in half and extending Layer 3 from the open aperture side. Radiation is then obtained by using a dominant slow-wave non-radiative SIW mode that excites a fast-wave higher-order ($n = -1$) space wave [20]. This is achieved by introducing a periodic structure along the length of the open waveguide. Subsequently, a high

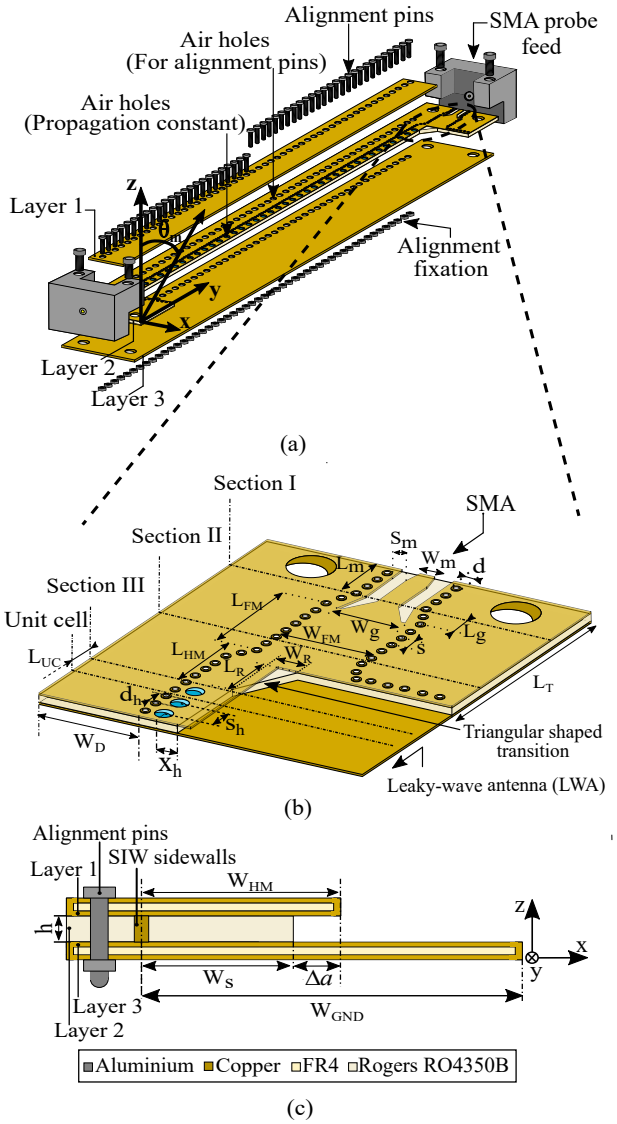

Fig. 1. Concept and architecture of the partially-filled HM-SIW LWA. (a) Exploded view. (b) Three-sections' transition from SMA probe to half-mode LWA. (c) Cross-sectional view. Optimized dimensions: W_m = 1 mm, S_m = 0.5 mm, L_m = 3.34 mm, W_g = 3.22 mm, L_g = 1.4 mm, W_{FM} = 4.42 mm, L_{FM} = 53.9 mm, W_s = 1.9 mm, L_{HM} = 3.7 mm, W_R = 1.32 mm, L_R= 2.83 mm, L_T = 11.24 mm, L_{UC} = 1.3 mm, Δa = 0.7 mm, W_D = 4.5 mm, W_{GND} = 10.5 mm, d_h = 1.1 mm, s_h = 1.3 mm, x_h = 0.9 mm, h = 0.5 mm, d = 0.4 mm, s = 0.8 mm.

directivity in the yz-plane and a typical fan beam in the xz-plane with frequency scanning are obtained.

To analyze the performance of the topology, the complex propagation constant of the leaky-wave modes propagating along the longitudinal direction (y-direction), with frequency ω and wave number $k_y(\omega)$, is considered. The dispersion relation of the leaky wave is

$$k_y(\omega) = \beta_y(\omega) - j\alpha_y(\omega), \tag{1}$$

where $\beta_y(\omega)$ and $\alpha_y(\omega)$ are the phase and leakage constant of the mode, respectively. To fix the cut-off frequency of the fundamental quasi-TE_{10} mode to 21 GHz, W_s=1.9 mm is obtained by the formula in [21] and the radiation is then adjusted by varying Δa [18]. Next, the diameter of the air holes [Fig. 1(b)] is set to d_h = 1.1 mm with an offset of x_h = 0.9 mm from the open side. Their center-to-center spacing

This article has been accepted for publication in a future issue of this journal, but has not been fully edited. Content may change prior to final publication. Citation information: DOI 10.1109/LAWP.2020.3038201, IEEE Antennas and Wireless Propagation Letters

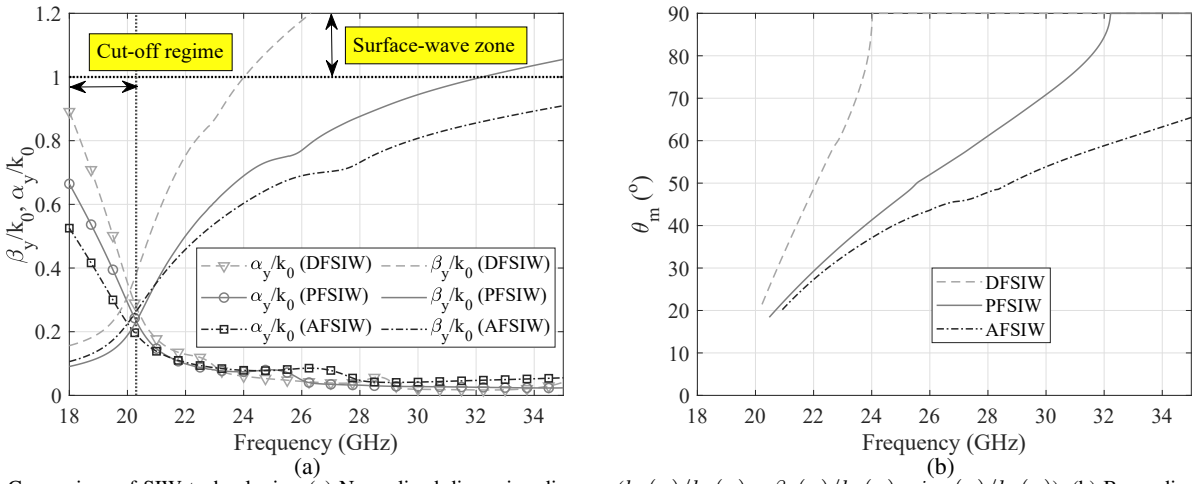

Fig. 2. Comparison of SIW technologies. (a) Normalized dispersion diagram ($k_y(\omega)/k_0(\omega) = \beta_y(\omega)/k_0(\omega) - j\alpha_y(\omega)/k_0(\omega)$). (b) Beam direction ($\theta_m$). Unit cell dimensions: DFSIW topology: L_{UC} = 1.3 mm, W_{HM} = 1.76 mm, W_s = 5 mm, Δa = 0 mm, W_{GND} = 5 mm, d = 0.4 mm, s = 0.8 mm; AFSIW topology: L_{UC} = 1.3 mm, W_{HM} = 3.41 mm, W_s = 0.3825 mm, Δa = 3.0275 mm, W_{GND} = 6.82 mm, d = 0.4 mm, s = 0.8 mm; PFSIW topology: L_{UC} = 1.3 mm, W_{HM} = 2.6 mm, W_s = 1.9 mm, Δa = 0.7 mm, d_h = 1.1 mm, s_h = 1.3 mm, x_h = 0.9 mm, W_{GND} = 10.5 mm, d = 0.4 mm, s = 0.8 mm.

equals s_h = 1.3 mm, which is the minimum value compatible with standard PCB manufacturing constraints in the RF-pool fabrication process at Eurocircuits [22]. Note that these air hole parameters (d_h, x_h and s_h) can be used to control the beam direction within the targeted frequency band. Yet, they do not alter the scanning range. Next, the relation (1) is determined by a CST Microwave Studio full-wave simulation of a single unit cell [Fig. 1(b)] and applying Bloch theory [23]. To obtain the desired radiated power fraction, $P\%$, the physical length of the antenna section, L, is calculated by [24]

$$P\% = 100\{1 - e^{-4\pi(\alpha_y(\omega)/k_0(\omega))(L/\lambda_0(\omega))}\}, \qquad (2)$$

where $k_0(\omega)$ is the free-space wave number and $\lambda_0(\omega)$ is the free-space wavelength. This yields an LWA composed of 77 unit cells, which remains electrically relatively small, featuring a length $L \approx 8\lambda$ without the feeding-line sections.

III. Comparison of SIW Topologies

For comparison, also half-mode LWAs in DFSIW and AFSIW technologies have been designed and optimized for the specified frequency band of operation. The DFSIW antenna is created on a single layer of Rogers 4350B substrate with a thickness of 0.5 mm, whereas the AFSIW is constructed by stacking a 0.5-mm-thick-Rogers 4350B substrate between 1.0-mm-thick-FR4 substrates, and by applying vias with 0.4 mm diameter and spaced by 0.8 mm to create an isolated half-mode air waveguide. Additionally, the width of the structures is implemented to fix the cut-off frequency of the fundamental mode at 21 GHz.

The radiation bandwidth of the leaky-wave antennas extends from the quasi-cut-off frequency, $|\alpha_y(\omega)/k_0(\omega)| \approx |\beta_y(\omega)/k_0(\omega)|$, to the surface-wave zone, $|\beta_y(\omega)/k_0(\omega)| \geq 1$. As seen in Fig. 2(a), the air-filled structure is superior with respect to radiation bandwidth than its dielectric-filled and partially-filled counterparts, since the normalized phase constant cannot approach the surface wave zone.

In terms of scan angle, the line $|\beta_y(\omega)/k_0(\omega)| = 1$ corresponds to end fire whereas $|\beta_y(\omega)/k_0(\omega)| = 0$ corresponds to broadside [Fig. 2(a)]. The $|\beta_y(\omega)/k_0(\omega)|$ variation near broadside is similar, independent from the dielectric filling factor of the wave guiding structure. Yet, significant differences occur near end fire. For the air-filled case, the beam direction varies little with frequency near the $|\beta_y(\omega)/k_0(\omega)| = 1$ line, since the dispersion curve asymptotically approaches that line for high frequencies. For the dielectric-filled and the partially-filled configurations, the dispersion curve easily covers the full spectral range between broadside and end fire within a finite frequency range. The curves quite rapidly approach and exceed the $|\beta_y(\omega)/k_0(\omega)| = 1$ line. Moreover, for the partially-filled structure, the scanning range [Fig. 2(b)] gradually enlarges when increasing the ratio of the dielectric width, W_s, over the upper conductor width, W_{HM}, [Fig. 1(c)]. Yet, for the air-filled structure, the beamwidth remains constant when the beam is scanned over a frequency range since the transverse wave number is constant, independent of frequency [24].

TABLE I
Performance Comparison of the Fabricated SIW LWAs at 24 GHz

Measured Figure of Merit	DFSIW	AFSIW	PFSIW
Bandwidth (GHz)	> 4	> 4	> 4
Realized gain (dBi)	11.6	15.0	15.5
Total antenna efficiency (%)	43.8	80	85
Scanning range (^{o})	49	9	20
Antenna length (mm)	160	80.6	126

The design target to radiate more than 80% power requires a long antenna aperture to leak the required power fraction all along its length. However, relying on air-filled or partially-filled configurations reduces the dielectric loss and increases the leakage rate, leading to high radiation efficiency in a shorter length.

To validate our partially-filled HM-SIW LWA and to demonstrate its potential, prototypes of the half-mode LWA in three different SIW technologies have been designed and fabricated by a standard PCB manufacturing process. Table I compares the measurement results. On the one hand, the partially-filled HM-SIW achieves a rather high radiation efficiency in a small footprint compared to the dielectric-filled topology. On the other hand, a much larger scanning range is obtained for the DFSIW

This article has been accepted for publication in a future issue of this journal, but has not been fully edited. Content may change prior to final publication. Citation information: DOI 10.1109/LAWP.2020.3038201, IEEE Antennas and Wireless Propagation Letters

TABLE II
PERFORMANCE COMPARISON OF PHASED-ARRAY ANTENNAS, OPERATING IN K-BAND

Ref.	[10]	[7]	[9]	[12]	[25]	[14]	[15]	This work
Scanning type	Mechanical movement	Phase shifter	Port switching	Port. switching	Frequency sweeping	Frequency sweeping	Frequency sweeping	Frequency sweeping
Bandwidth (GHz)	1.1	2	2	1	1	2	3	4
Peak gain (dBi)	22	9.9	-	22.6	10.7	14	13.5	15.7
Efficiency (%)	55	-	50	-	-	$\leq$ 30	-	$\geq$ 80
Scanning range (^{o})	35	45	30	33	9	10	15	20
Number of ports	1	1	5	5	1	2	2	2
Number of RF layers	2	1	2	3	1	1	1	1
Antenna size (mm^2)	190 x 170	$\sim$54 x 55	75 x 84	130 x 100	$\sim$126 x 15	186 x 28	-	126 x 15

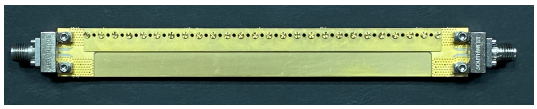

Fig. 3. Fabricated LWA prototype with end-launch connectors (electrical length approximately 10.3λ).

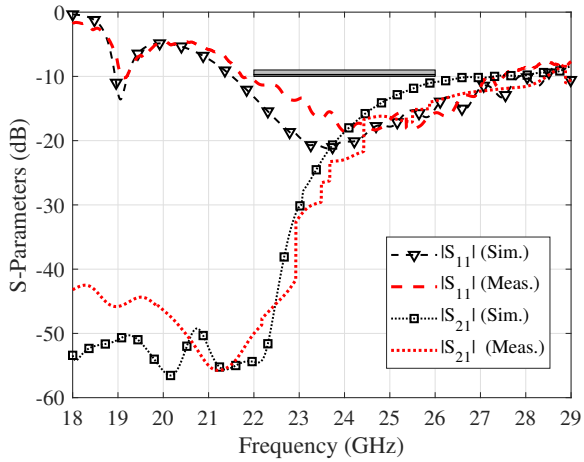

Fig. 4. Measured and simulated S-parameters of the partially-filled HM-SIW LWA.

compared to the AFSIW topology. It is clear that the topology advocated in this letter provides an excellent alternative to its dielectric- and air-filled counterparts.

IV. EXPERIMENTAL VALIDATION

The fabricated prototype of the partially-filled HM-SIW LWA is depicted in Fig. 3. The S-parameters are measured with an Agilent E8364B PNA Microwave Network Analyzer and solder-free K-type (2.92 mm) End-Launch connectors by Southwest Microwave [26]. The far-field measurements of the antenna are performed using an NSI-MI spherical near-field measurement range [27]. An ANT-SGH-22-33 standard gain horn [28] is used to determine the antenna gain. For adequate comparison between measured and simulated antenna performance, a model of the measurement connector is included in all simulations.

The measured S-parameters are shown in Fig. 4, along with the full-wave simulation results. A measured impedance bandwidth of 6.9 GHz is obtained from 22 GHz to 28.9 GHz, thereby covering the entire [22–26] GHz band.

Fig. 5 depicts the measured and simulated radiation patterns from 22 GHz to 26 GHz with a 2 GHz step. The main-beam angle varies from 38^o to 58^o. The measured realized peak gain and total antenna efficiency vary from 13.7 to 15.7 dBi and 95% to 80%, respectively. Moreover, at 24 GHz, a front-to-back ratio

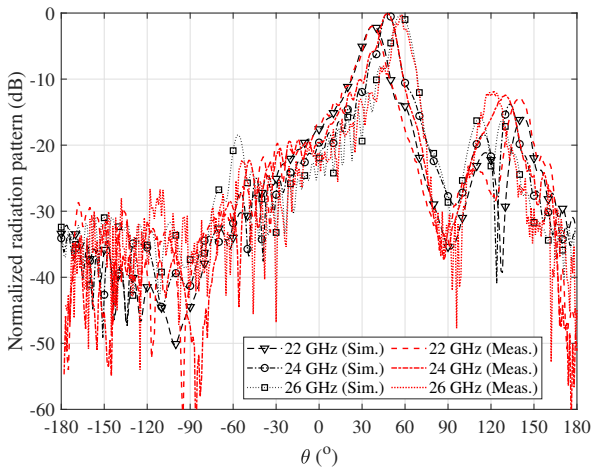

Fig. 5. Radiation patterns of the partially-filled HM-SIW LWA in yz-plane.

of 12 dB and a half power beamwidth of 10.2^o are obtained. Furthermore, the front-to-back ratio can be increased to 18 dB by enlarging the ground plane width, W_{GND}, to 12 mm. In general, we observe an excellent agreement between the simulated and measured radiation patterns, with a beam direction that slightly differs from that of the infinite periodic leaky-wave antenna because of the prototype's finite dimensions.

Finally, in Table II our partially-filled HM-SIW LWA is compared with other reported topologies in open literature. It is clear that our topology yields a large impedance bandwidth and high antenna efficiency while maintaining a small footprint, low profile, and compatibility with cost-efficient standard PCB processing. Moreover, our antenna topology provides cost effective frequency scanning over a wide angular range.

V. CONCLUSION

A novel LWA implemented in stacked PFSIW technology is proposed. The antenna features excellent performance, including compact size, easy fabrication, low cost, high efficiency, and wide bandwidth. Measurements reveal that the LWA exhibits a total antenna efficiency over 80%, a minimal boresight gain of 13.7 dBi, and sufficient bandwidth to cover the [22–26] GHz band. Moreover, the compact antenna footprint (15x126 mm^2) and high antenna-to-integration platform isolation make the developed antenna with beam-steering capabilities suitable for seamless installation on land vehicles for radar applications. Furthermore, given that the main beam only shifts by 1^o when sweeping over a bandwidth of 250 MHz, the proposed antenna may be applied in both frequency-modulated continuous-wave (FMCW) and pulsed radars.

REFERENCES

[1] W. Menzel and A. Moebius, "Antenna concepts for millimeter-wave automotive radar sensors," *Proceedings of IEEE*, vol. 100, no. 7, pp. 2372–2379, July 2012.

[2] V. Rabinovich and N. Alexandrov, *Antenna arrays and automotive applications*. Springer Science, 2013, ch. 1, pp. 1–20.

[3] F. Parment, A. Ghiotto, T. Vuong, J. Duchamp, and K. Wu, "Air-filled substrate integrated waveguide for low loss and high power handling millimeter-wave substrate integrated circuits," *IEEE Trans. Microw. Theory Tech.*, vol. 63, no. 4, pp. 1228–1238, Apr. 2015.

[4] C. Tomassoni, L. Silvestri, A. Ghiotto, M. Bozzi, and L. Perregrini, "A novel class of substrate integrated waveguide filters based on dual-mode air-filled resonant cavities," *IEEE Trans. Microw. Theory Tech.*, vol. 66, no. 2, pp. 726–736, Feb. 2018.

[5] L. Silvestri, A. Ghiotto, C. Tomassoni, M. Bozzi, and L. Perregrini, "Partially air-filled substrate integrated waveguide filters with full control of transmission zeros," *IEEE Trans. Microw. Theory Tech.*, vol. 67, no. 9, pp. 3673–3682, Sep. 2019.

[6] A. Coves, G. Torregrosa, G. Vicent, E. Bronchalo, A. A. San Blas, and M. Bozzi, "Modeling of perforated SIW structures and their application to the design of step-impedance microwave filters," in *Proc. IEEE MTT-S International Conference on Numerical Electromagnetic and Multiphysics Modeling and Optimization for RF, Microwave, and Terahertz Applications (NEMO)*, Seville, Spain, May 2017, pp. 293–295.

[7] R. A. Alhalabi and G. M. Rebeiz, "High-efficiency angled-dipole antennas for millimeter-wave phased array applications," *IEEE Trans. Antennas Propag.*, vol. 56, no. 10, pp. 3136–3142, October 2008.

[8] S. Otto, A. Al-Bassam, A. Renning, K. Solbach, and C. Caloz, "Radiation efficiency of longitudinally symmetric and asymmetric periodic leaky-wave antennas," *IEEE Antennas and Wireless Propag. Lett.*, vol. 11, pp. 612–615, 2012.

[9] W. Lee, J. Kim, and Y. J. Yoon, "Compact two-layer Rotman lens-fed microstrip antenna array at 24 GHz," *IEEE Trans. Antennas Propag.*, vol. 59, no. 2, pp. 460–466, February 2011.

[10] E. Gandini, M. Ettorre, M. Casaletti, K. Tekkouk, L. Le Coq, and R. Sauleau, "SIW slotted waveguide array with pillbox transition for mechanical beam scanning," *IEEE Antennas and Wireless Propag. Lett.*, vol. 11, pp. 1572–1575, 2012.

[11] K. Tekkouk, M. Ettorre, and E. a. Gandini, "Multibeam pillbox antenna with low sidelobe level and high-beam crossover in SIW technology using the split aperture decoupling method," *IEEE Trans. Antennas Propag.*, vol. 63, no. 11, pp. 5209–5214, November 2015.

[12] K. Tekkouk, M. Ettorre, L. Le Coq, and R. Sauleau, "Multibeam SIW slot waveguide antenna system fed by a compact dual-layer Rotman lens," *IEEE Trans. Antennas Propag.*, vol. 64, no. 2, pp. 504–514, February 2016.

[13] K. Tekkouk, M. Ettorre, and R. Sauleau, "SIW Rotman lens antenna with ridged delay lline and reduced footprint," *IEEE Trans. Microw. Theory Tech.*, vol. 66, no. 6, pp. 3136–3144, June 2018.

[14] O. Bayraktar and O. A. Civi, "Circumferential travelling wave slot array on cylindrical substrate integrated waveguide (CSIW)," *IEEE Trans. Antennas Propag.*, vol. 62, no. 7, pp. 3557–3566, July 2014.

[15] W. Cao, Z. N. Chen, W. Hong, B. Zhang, and A. Liu, "A beam scanning leaky-wave slot antenna with enhanced scanning angle range and flat gain characteristic using composite phase-shifting transmission line," *IEEE Trans. Antennas Propag.*, vol. 62, no. 11, pp. 5871–5875, Nov 2014.

[16] J. Xu, W. Hong, H. Tang, Z. Kuai, and K. Wu, "Half-mode substrate integrated waveguide (HMSIW) leaky-wave antenna for millimeter-wave applications," *IEEE Antennas and Wireless Propag. Lett.*, vol. 7, pp. 85–88, 2008.

[17] FCC, "Revision of part 15 of the commission's rules regarding ultra wideband transmission systems," fed. Commun. Commiss., First Report and Order, ET Docket 98-153, FCC 02-48, Adopted Feb. 14, 2002, Released Apr. 22, 2002.

[18] I. S. S. Lima, F. Parment, A. Ghiotto, T.-P. Vuong, and K. Wu, "Broadband dielectric-to-half-mode air-filled substrate integrated waveguide transition," *IEEE Microwave and Wireless Components Lett.*, vol. 26, no. 6, pp. 383–385, Jun. 2016.

[19] P. Vartanian, W. Ayres, and A. Helgesson, "Propagation in dielectric slab loaded rectangular waveguide," *IRE Trans. Microw. Theory Tech.*, vol. 6, no. 2, pp. 215–222, April 1958.

[20] W. Rotman and A. Oliner, "Periodic structures in trough waveguide," *IRE Trans. Microw. Theory Tech.*, vol. 7, no. 1, pp. 134–142, Jan. 1959.

[21] Q. Lai, C. Fumeaux, W. Hong, and R. Vahldieck, "Characterization of the propagation properties of the half-mode substrate integrated waveguide," *IEEE Trans. Microw. Theory Tech.*, vol. 57, no. 8, pp. 1996–2004, Aug. 2009.

[22] Eurocircuits. (2015). RF pool – all the benefits of pooling on RF materials [Online]. Available: http://www.eurocircuits.com/rf-pool-allthe-benefits-of-pooling-on-rf-materials/.

[23] R. E. Collin, *Field Theory of Guided Waves*, 1st ed. WcGraw-Hill, 1960, ch. 9, pp. 368–408.

[24] A. A. Oliner and D. R. Jackson, *Leaky-wave antennas, [in Antenna Engineering Handbook]*. New York: McGraw-Hill, 2007, ch. 11, pp. 286–342.

[25] M. Kuznetcov, V. Gomez-Guillamon Buendia, Z. Shafiq, L. Matekovits, D. Anagnostou, and S. K. Podilchak, "Printed leaky-wave antenna with aperture control using width-modulated microstrip lines and TM surface-wave feeding by SIW technology," *IEEE Antennas and Wireless Propag. Lett.*, vol. 18, no. 9, pp. 1809–1813, Sep. 2019.

[26] Southwest Microwave, Inc. (2016). 1.85 mm (V) DC to 67.0 GHz Connectors [Online]. Available: http://mpd.southwestmicrowave.com.

[27] NSI–MI Technologies (2017). Spherical Near-Field Scanner Systems. [Online]. Available: https://www.nsi-mi.com.

[28] NSI-MI Technologies Standard Gain Horns - [Online]. Available: https://www.nsi-mi.com/images/PDF_Datasheets/NSI-MI-ANT-SGH-Standard-Gain-Horns-v1.3.pdf.